Balestrieri, C., Colonna, G., & Irace, G. (1973) *Comp. Biochem. Physiol., B: Comp. Biochem. 46B*, 667–672.
Balestrieri, C., Colonna, G., Giovane, A., Irace, G., & Servillo, L. (1976) *FEBS Lett. 66*, 60–64.
Balestrieri, C., Colonna, G., Giovane, A., Irace, G., & Servillo, L. (1978a) *Eur. J. Biochem. 90*, 433–440.
Balestrieri, C., Colonna, G., Giovane, A., Irace, G., Servillo, L., & Tota, B. (1978b) *Comp. Biochem. Physiol., B: Comp. Biochem. 60B*, 195–199.
Balestrieri, C., Colonna, G., Giovane, A., Irace, G., & Servillo, L. (1980) *Anal. Biochem. 106*, 49–54.
Bismuto, E., Colonna, G., Savy, F., & Irace G. (1985) *Int. J. Pept. Protein Res. 26*, 195–207.
Colonna, G., Balestrieri, C., Bismuto, E., Servillo, L., & Irace, G. (1982) *Biochemistry 21*, 212–215.
Creighton, T. E. (1985) *J. Phys. Chem. 89*, 2452–2459.
Dayhoff, M. O. (1972) *Atlas of Protein Sequence and Structure*, Vol. 5, National Biomedical Research Foundation, Washington, DC.
Donovan, J. W. (1969) in *Physical Principles and Techniques of Protein Chemistry* (Leach, S. J., Ed.) Part A, pp 101–170, Academic, New York.
Fosmiri, G. J., & Brown, W. D. (1976) *Comp. Biochem. Physiol., B: Comp. Biochem. 55B*, 293–299.
Irace, G., Bismuto, E., Savy, F., & Colonna, G. (1986) *Arch. Biochem. Biophys. 244*, 459–469.
Kuntz, I. D. (1975) *J. Am. Chem. Soc. 97*, 4362–4366.
Lee, B., & Richards, F. M. (1971) *J. Mol. Biol. 55*, 370–400.
Ragone, R., Colonna, G., Balestrieri, C., Servillo, L., & Irace, G. (1984) *Biochemistry 23*, 1871–1875.
Ragone, R., Colonna, G., Servillo, L., & Irace, G. (1985) *Photochem. Photobiol. 42*, 505–508.
Rossmann, M. G., & Argos, P. (1975) *J. Biol. Chem. 250*, 7525–7532.
Servillo, L., Colonna, G., Ragone, R., Irace, G., & Balestrieri, C. (1980) *Ital. J. Biochem. 29*, 449–450.
Servillo, L., Colonna, G., Balestrieri, C., Ragone, R., & Irace, G. (1982) *Anal. Biochem. 126*, 251–257.
Takano, T. (1977) *J. Mol. Biol. 110*, 535–568.
Teale, F. W. J. (1959) *Biochim. Biophys. Acta 35*, 543.
Watts, D. A., Rice, R. H., & Brown, D. B. (1980) *J. Biol. Chem. 255*, 10916–10924.
Wetlaufer, D. B. (1962) *Adv. Protein Chem. 17*, 303–390.
Wetlaufer, D. B. (1973) *Proc. Natl. Acad. Sci. U.S.A. 70*, 697–701.
Wodak, S. J., & Janin, J. (1981) *Biochemistry 20*, 6544–6552.

Secondary Structure Determination in Proteins from Deep (192–223-nm) Ultraviolet Raman Spectroscopy†

Robert A. Copeland and Thomas G. Spiro*
Department of Chemistry, Princeton University, Princeton, New Jersey 08544
Received September 9, 1986; Revised Manuscript Received December 12, 1986

ABSTRACT: Raman intensities obtained with UV laser excitation at 223, 218, 204, 200, and 192 nm are reported for the amide I, II, III, and II′ bands of random-coil polylysine. The excitation profiles show enhancement via the π–π^* electronic transition, at ~190 nm. Enhancement for amide I is weak, however, and most of the intensity can be accounted for by preresonance with a deeper UV transition at ~165 nm. The amide II′ band dominates the spectrum in D_2O, consistent with the suggestion that the main distortion coordinate in the π–π^* excited state is the stretching of the C–N peptide bond. Amide II intensities with 200- and 192-nm excitation are reported for several proteins. The previously reported negative linear correlation with α-helix content (due to Raman hypochromism in the α-helices) is found not to apply to proteins with high β-sheet content when the excitation wavelength is 200 nm. Much higher intensities are seen for these proteins and are attributed to a red shift of the π–π^* absorption for the β-structure. A linear correlation with α-helix content is found for excitation of 192 nm, which corresponds to an isosbestic point of the β-sheet and random-coil absorption bands. Characteristic amide II Raman cross sections are derived for α-helical, β-sheet, and random-coil elements and are used to determine secondary structure for α_1- and β-purothionin, by use of amide II intensities with 200- and 192-nm excitation. The results are in good agreement with a previous determination based on amide I band deconvolution in off-resonance Raman spectra.

The amide linkage is the fundamental structural component of all proteins and polypeptides. Differences in inter-amide hydrogen bonding are the basis for the diversity of protein structure exhibited in nature (Creighton, 1983). This H bonding stabilizes well-ordered (secondary) structures (e.g., α-helix and β-sheet) where the proximity and orientation of adjacent amides lead to significant dipolar interactions (Creighton, 1983). Such interactions influence several spectroscopic probes, which can be used to monitor secondary structure (Cantor & Schimmel, 1980).

Ultraviolet (UV) circular dichroism is perhaps the most widely used method for secondary structure determinations in proteins (Cantor & Schimmel, 1980). Although this technique has proved reliable in many cases, ambiguities can arise from non-amide chiral chromophores within proteins (Campbell & Dwek, 1984; Walton, 1981). Aromatic amino acids, arginine residues, and prosthetic groups can interfere with the circular dichroism determinations. Nonresonance Raman (Frushour & Koenig, 1975; Lippert et al., 1976;

† This work was supported by NIH Grant GM 25158.
* Author to whom correspondence should be addressed.

0006-2960/87/0426-2134$01.50/0

Parker, 1983; Williams, 1983) and infrared (Byler et al., 1986) spectroscopies have increasingly been applied to secondary structure determination, although these methods require high protein concentrations because of their low sensitivity. NMR spectroscopy provides the most detailed information about protein structure (Billeter et al., 1982; Wand & Englander, 1986a,b) but requires extensive analysis and is limited to relatively small proteins.

In the far-UV region the amide π-electron system gives rise to a strong absorption band at ca. 190 nm (Cantor & Schimmel, 1980). Doty and co-workers have shown the intensity of this band to be a marker of secondary structure in homopolypeptides and proteins; the band is significantly hypochromic for α-helices and slightly hyperchromic and red shifted for β-sheet structure relative to random-coil forms (Rosenheck & Doty, 1961). Tinoco and co-workers have explained these changes in terms of constructive (β-sheet) and destructive (α-helix) transition dipole interactions of adjacent amide linkages (Tinoco et al., 1962). Far-UV absorption spectroscopy, however, is *not* a convenient method for the determination of protein secondary structure because of interferences from the overlapping absorptions of the aromatic amino acids and other protein components (Wetlaufer, 1962). Recently, several groups have turned their attention to UV resonance Raman (UVRR) spectroscopy as a means of studying structure in model amides and proteins (Chinsky et al., 1985; Copeland et al., 1985; Copeland & Spiro, 1985, 1986; Dudik et al., 1985a; Johnson et al., 1984; Mayne et al., 1985; Rava & Spiro, 1985). Due to the resonance enhancement, UVRR spectroscopy is applicable at far lower concentrations than visible excitation Raman spectroscopy (although the amounts of material required are similar because of the need to circulate the UVRR sample to avoid thermal and photoinduced damage), and nonprotein components of the sample (e.g., lipids, buffers) do not interfere. Moreover, interference from fluorescent components or impurities, which is a major problem in visible excitation studies, is avoided in UVRR spectroscopy since the excitation and scattered light are at wavelengths far below the fluorescence spectra that are commonly encountered.

We have demonstrated that UVRR spectroscopy, with excitation at 200 nm, can discriminate between secondary structure components in proteins on the basis of amide vibrational-mode hypochromism associated with α-helices (Copeland & Spiro, 1986). Linear correlations were established between the α-helix fraction and the Raman intensity of the amide II, II′ (in D_2O), and III modes in proteins with only α-helix and random-coil components. In this study we find that proteins with substantial β-sheet structure give higher than predicted intensities, an effect attributable to the red shift of the β π–π^* absorption. When, however, the amide II intensity is determined with 192-nm excitation, the β-containing proteins follow the same linear correlations with α-helix content as other proteins. This wavelength is isosbestic for β-sheet and random-coil polypeptides. It is therefore possible to determine all three major elements of secondary structure with intensities determined at both 200 and 192 nm. Raman cross sections appropriate to this determination are derived from the available protein data. There are, of course, other secondary structure elements, such as β-turns, which are of considerable interest, and one would like to know whether β-sheet segments are parallel or antiparallel. These more subtle aspects of secondary structure are unlikely to be differentiated by intensity measurements alone and will require more careful analysis of band contours than the presently available signal/noise of UVRR spectra can support.

We also report excitation profiles for the homopolypeptide poly(L-lysine) in the random-coil form, from 223 to 192 nm. They support the inference (Mayne et al., 1985) that those modes with significant C–N stretching character (i.e., amide II, II′, and III) gain intensity from the ~190-nm π–π^* transition. The amide I (mostly C=O stretching) mode, however, appears to gain most of its UV Raman intensity via preresonance enhancement from a higher lying n–σ^* transition at ca. 165 nm (Bensing & Pysh, 1969; Momii & Urry, 1968; Onary, 1970). This result helps explain the facts that the amide I mode for α-helices is not significantly hypochromic when excited in the UV (Copeland & Spiro, 1986) and is actually hyperchromic when excited in the visible region (Painter & Koenig, 1976).

Experimental Procedures

Poly(L-lysine), equine heart cytochrome *c*, sperm whale myoglobin, rabbit muscle tropomyosin, and bovine insulin were purchased from Sigma and used as received. α_1- and β-purothionin were gifts from Dr. F. G. Prendergast, Department of Pharmacology, Mayo Medical School. Bovine superoxide dismutase was a gift from Dr. J. Valentine, Department of Chemistry, University of California at Los Angeles. Samples of the lyophylized proteins were dissolved (200 μM) in 0.05 M phosphate buffer (pH 7) containing 0.4 M sodium sulfate as an intensity standard for Raman spectroscopy. Insulin samples were prepared at pH 10 in order to obtain monomeric protein (Rava & Spiro, 1985). Poly(L-lysine) was dissolved in 1 M phosphate buffer (pH/pD 5) to a concentration of 0.6 mM in peptide units. A Raman band of phosphate (~1075 cm^{-1}) was used as an intensity standard in this case. Sample pH values were measured with a Corning Model 150 pH meter. For samples in D_2O, the pD values were corrected for the deuterium isotope effect (Glasoe & Long, 1960).

Raman spectra were obtained with excitation wavelengths from 223 to 192 nm produced by H_2 shifting of the frequency-doubled (532 nm), -tripled (355 nm), and -quadrupled (266 nm) output of a Nd:YAG laser, with the experimental arrangement described by Fodor et al. (1986). Spectra were signal averaged over 8–20 scans to develop adequate signal. Sample solutions were replaced after every second or third scan to avoid laser-induced damage.

Absolute Raman cross sections were determined from the ratio of peak heights (measured against a base line connecting points on either side of the band) of the sample and of the intensity standard by the relation (Dudik et al., 1985b)

$$\sigma_N = \sigma_S \left[\frac{I_N}{I_S} \frac{C_S}{C_N} \frac{(\nu_0 - \nu_S)}{(\nu_0 - \nu_N)} \right] \quad (1)$$

where σ_N is the absolute Raman cross section per mole of peptide for the sample vibrational mode, σ_S is the absolute Raman cross section for the standard vibrational mode, I_N and I_S are the peak intensities for the sample and standard Raman bands, respectively, ν_0 is the laser excitation frequency, ν_N and ν_S are the vibrational frequencies (Δcm^{-1}) of the sample and standard Raman bands, and C_N and C_S are the molar concentrations of sample (in terms of peptide bonds) and standard, respectively. The values of σ_S for the sulfate ν_1 band were determined (Fodor et al., 1987) relative to the Rayleigh scattering intensity of standard $BaSO_4$ particles as described by Dudik et al. (1985b). Phosphate σ_S values were determined relative to sulfate.

The absorption spectrum of random-coil poly(L-lysine) (Figure 1) was obtained with a nitrogen-purged (~5 h) Cary 118 UV–vis spectrophotometer. The sample and reference

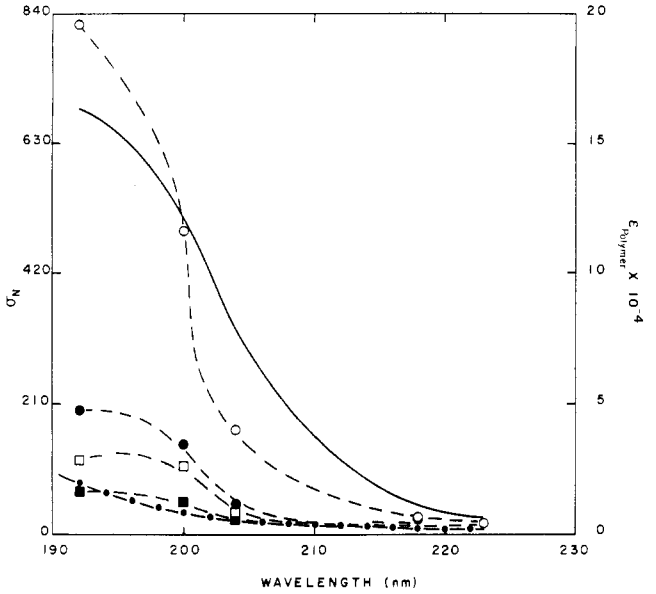

FIGURE 1: UV absorption spectrum (solid line) of random-coil polylysine (pH/pD 5) and Raman excitation profiles for the amide I (■), II (●), III (□), and II′ (○) bands. The solid dotted curve at the bottom of the figure is the predicted *A* term preresonance behavior, assuming resonance with a 165-nm transition, scaled to the amide I intensity at 223 nm.

buffers were contained in matched 0.1-cm fused silica cells.

Results and Discussion

Polylysine Excitation Profiles. The amide II mode of peptides is very weak in Raman spectra excited with visible excitation but is strongly enhanced by resonance with the ~190-nm amide allowed electronic transition (Mayne et al., 1985; Copeland & Spiro, 1986). Even at 257 nm its enhancement is evident (Sugawara et al., 1978), and it becomes one of the most prominent features in Raman spectra of proteins excited at 200 (Rava & Spiro, 1985) and 192 nm (Fodor et al., 1986). The amide II and III modes, at ~1550 and ~1250 cm^{-1}, are mixtures of C–N stretching and N–H bending coordinates, primarily (Harada & Takeuchi, 1986). When the amide N–H proton is exchanged for a deuteron, the N–D bending mode is at much lower frequency, leaving amide II′, at ~1460 cm^{-1}, as a nearly pure C–N stretching mode. Mayne et al. (1985) showed that dissolution of *N*-methylacetamide in D_2O produces a pronounced intensification of the amide II′ band, which completely dominates the 218-nm-excited spectrum, implying that C–N stretching is the main distortion coordinate in the amide π–π^* excited state. The enhancement of the amide I mode, which is mainly C–O stretching in character, was much weaker. Dudik et al. (1985a) determined the excitation profile for *N*-methylacetamide and related molecules between 560 and 220 nm and showed that there was no detectable influence of the weak amide n–π^* transition at ~220 nm on the Raman intensities.

These conclusions are supported by our excitation profiles, shown in Figure 1, for polylysine in H_2O and D_2O, at pH/pD 5, when it is in a random-coil conformation (Sugawara et al., 1978). The amide I (1660 cm^{-1}), II (1560 cm^{-1}), and III (1260 cm^{-1}) intensities, as well as the amide II′ (1475 cm^{-1}) intensity in D_2O, rise smoothly through the 240–192-nm region, tracking the absorption spectrum. The Raman intensity scales roughly with the square of the absorptivity. For example, the intensities are ~4-fold higher while the absorptivity is ~2-fold higher at 192 than at 204 nm. The amide II′ intensity is substantially higher than the sum of the amide II and III intensities. In part, this is an artifact of the use of peak heights

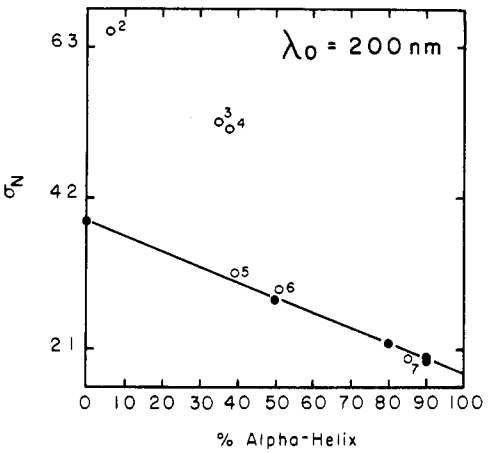

FIGURE 2: Plot of amide II Raman cross sections with 200-nm excitation vs. percent α-helix. Solid circles are for tropomyosin at pH values between 7.0 and 12.5 (Copeland & Spiro, 1986). Open circles are for the proteins: (2) superoxide dismutase; (3) β-purothionin; (4) α_1-purothionin; (5) cytochrome *c*; (6) insulin, pH 10; (7) myoglobin.

in the intensity measurements, since the amide III band is broader than the amide II and II′ bands. There are many modes of a polypeptide in the 1200–1400-cm^{-1} region among which N–H bending and C–N stretching coordinates are distributed (Krimm & Bandkar, 1986). The very large (factor of ~4) intensification of amide II′ with respect to amide II, however, suggests that there may be some intensity cancellation in the amide II mode due to the relative phasing of the internal coordinate contributors.

The amide I enhancement is weak, as noted previously (Mayne et al., 1985; Copeland & Spiro, 1986). In Figure 1 the amide I intensities are compared with the expected behavior due to preresonance with an electronic transition at 165 nm. This is the wavelength of the next major amide absorption band and has been assigned to a n → σ^* transition (Peterson & Simpson, 1957). The *A* term preresonance equation (Trulson & Mathies, 1986)

$$\sigma_N = K(\nu_0 - \nu_N)^4 \left[\frac{\nu_e^2 + \nu_0^2}{(\nu_e^2 - \nu_0^2)^2} \right]^2 \quad (2)$$

was used in this calculation and scaled to the experimental intensity at 223 nm. Here, ν_e is the frequency of the preresonant electronic transition and *K* is a constant related to the coupling strength (Trulson & Mathies, 1986). This equation describes the data quite well, with only a slight deviation being evident at 200 nm.

The lack of significant enhancement for amide I via the first π–π^* transition accounts for the absence of α-helical hypochromism for the amide I band when measured at 200 nm (Copeland & Spiro, 1986). This band is actually *hyper*chromic when measured with visible-wavelength excitation. Although Painter and Koenig (1976) had suggested enhancement via the n–π^* transition (~220 nm) to account for this effect, the present observation of preresonance enhancement via the 165-nm band supports our previous suggestion (Copeland & Spiro, 1986) that the off-resonance hyperchromism is associated with the known absorption hyperchromism (Bensing & Pysh, 1969; Momii & Urry, 1968; Onari, 1970) of higher electronic transitions (~165 nm) in α-helical polypeptides.

Amide II Intensities at 200 and 192 nm. Table I lists amide II (1560 cm^{-1}) and I (1660 cm^{-1}) intensities for several proteins when excited at 200 and 192 nm. Figure 2 is a plot of the 200-nm amide II data against α-helix content. The straight

Table I: Absolute Raman Cross Sections, σ_N (millibarns/molecule steradian), for the Amide I and II Modes of Proteins with Variable Secondary Structure with 200- and 192-nm Excitation[a]

	λ_0 192 nm		λ_0 200 nm		reported secondary structure (%)			
sample	amide II	amide I	amide II	amide I	α	β	τ	ref
tropomyosin, pH 7	71	63	20	16	90	0	10	Lowey, 1965
myoglobin	80	50	21	16	86	0	14	Dickerson & Geis, 1983
insulin, pH 10	85	46	29	17	51	12	37	Blundell et al., 1972
cytochrome *c*	103	69	31	17	39	0	61	Dickerson et al., 1971
α_1-purothionin	106	69	51	33	38	29	33	Williams & Teeter, 1984
β-purothionin	102	75	52	33	35	31	34	Williams & Teeter, 1984
superoxide dismutase	117	52	94	33	6	50	44	Richardson et al., 1975
tropomyosin, pH 12.5	133	51	38	17	0	0	100	Lowey, 1965

[a] Standard amide II cross sections: at λ_0 192 nm, $\sigma_\alpha = 66$ and $\sigma_\beta = \sigma_\tau = 125$, obtained by linear regression with percent α-helix (Figure 4) for all samples except the purothionins; at λ_0 200 nm, $\sigma_\alpha = 18$ and $\sigma_\tau = 38$, obtained by linear regression with percent α-helix (Figure 3) for tropomyosin at various pH values [see Copeland & Spiro (1986)] and $\sigma_\beta = 94$, obtained by difference with superoxide dismutase.

line, reported in our earlier study (Copeland & Spiro, 1986), connects points for tropomyosin at pH 7 where it is 90% α-helical and at higher pH values where it is progressively converted to a random-coil structure (Lowey, 1965). Other proteins, myoglobin (Dickerson & Geis, 1983) and cytochrome *c* (Dickerson et al., 1971), which contain only α-helices and unordered segments, and insulin (Blundell et al., 1972), which contains a small β-sheet contribution, also fall on the line. However, proteins with substantial β-sheet content, superoxide dismutase (Brahms & Brahms, 1980; Richardson et al., 1975) and α_1- and β-purothionin (Williams & Teeter, 1984), deviate widely from the line, giving much higher than predicted amide II intensities.

Figure 3 shows UV absorption spectra for α-helical, β-sheet, and random-coil polypeptides, as determined by Rosenheck and Doty (1961). The absorption is substantially lower for the α-helix than for the other structures, due to a hypochromic interaction of neighboring transition dipoles (Tinoco et al., 1962). This is the basis of the α-helical UVRR hypochromism that is responsible for the correlation shown in Figure 2. The β-sheet spectrum shows a slight hyperchromism and red shift relative to the random-coil spectrum. The absorption hyperchromism is too small to account for the large deviations shown by the UVRR intensities of the β-sheet-containing proteins. The Raman hyperchromic ratio is expected to be equal to the square of the absorption hyperchromic ratio, all factors other than the absorption strength being equal (Copeland & Spiro, 1986). From the β-sheet/random-coil absorptivity ratio of 1.1, measured at the absorption maxima, one expects a Raman intensity ratio of 1.2. Yet, the deviant points in Figure 2 exceed the predicted values by factors of $\sim$1.7. The major part of these deviations is therefore attributable to the β-sheet absorption red shift, which brings the 200-nm excitation closer to resonance with the π–π^* transition and significantly increases the enhancement.

Figure 3 shows that the β-sheet and random-coil absorptivities are equal at 192 nm. Reasoning that their Raman intensities might also be equal at this wavelength, we determined amide II intensities for the same set of proteins using 192-nm excitation. The results plotted in Figure 4 show another linear correlation with α-helix content that now holds for proteins with or without significant β-segments, thus confirming the hypothesis. As with 200-nm excitation (Copeland & Spiro, 1986), the amide I intensities (see Table I) show no significant correlation with α-helical content and indeed show a rather wide scatter.

Since the β-sheet contribution is so different at 200 and 192 nm, it is possible to use the amide II intensity at both wavelengths to determine all three principal elements of secondary structure. At each wavelength the composite amide II cross

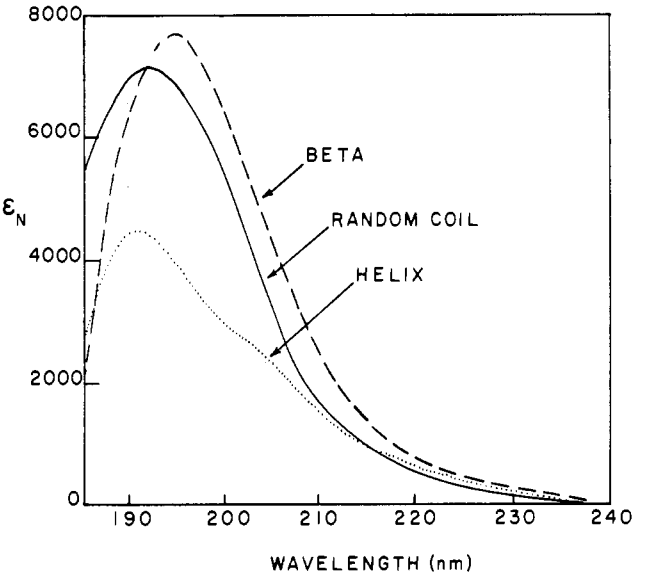

FIGURE 3: Absorption spectra for polylysine in α-helical, β-sheet, and random-coil conformations, from Rosenheck and Doty (1961).

section (per mole of peptide) can be divided into three contributions:

$$\sigma_N = f_\alpha\sigma_\alpha + f_\beta\sigma_\beta + f_\tau\sigma_\tau \quad (3)$$

where σ_α, σ_β, and σ_τ are cross sections characteristic of α-helix, β-sheet, and random-coil structure and f_α, $f\beta$, and f_τ are their mole fractions in the protein. This division implies that all unordered segments have random-coil cross sections, a reasonable approximation supported by the data. Since the mole fractions sum to unity, all three can be determined from intensity measurements at two wavelengths, provided the σ_α, σ_β, and σ_τ values are known. We determined these values at 192 nm by a least-squares fit of the best straight line in Figure 4 assuming $\sigma_\beta = \sigma_\tau$, as implied by the data. At 200 nm, σ_α and σ_τ were determined by a least-squares fit of the line in Figure, while σ_β was determined by difference from the intensity for superoxide dismutase, whose crystal structure is known (Richardson et al., 1975). The results are given in Table I.

We used these standard cross sections to determine the secondary structure for α_1- and β-purothionin. Other aspects of the UV Raman spectra of these proteins will be published separately (R. A. Copeland, F. G. Prendergast, and T. G. Spiro, unpublished results). These proteins have been studied by Raman spectroscopy with visible excitation, and the elements of secondary structure were estimated by deconvoluting the amide I band into standard components (Williams & Teeter, 1984). Comparable amounts of α-helix, β-sheet, and unordered segments were found. The agreement between our

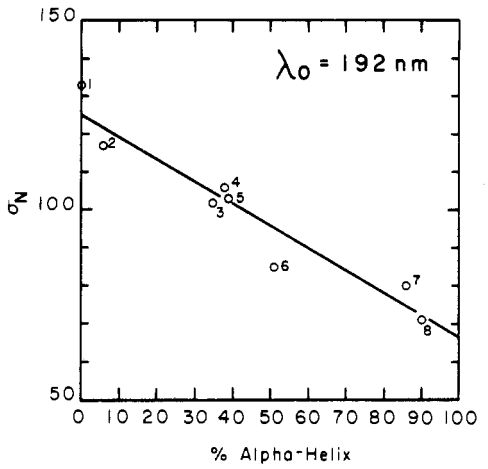

FIGURE 4: Plot of amide II Raman cross sections with 192-nm excitation vs. percent α-helix for the following: (1) tropomyosin, pH 12.5; (2) superoxide dismutase; (3) β-purothionin; (4) α_1-purothionin; (5) cytochrome *c*; (6) insulin, pH 10; (7) myoglobin; (8) tropomyosin, pH 7.0.

Table II: Calculated Secondary Structure Composition for the Purothionins

	UVRR amide II intensity (this work)		visible Raman amide I deconvolution (Williams & Teeter, 1984)	
	% α	% β	% α	% β
α_1-purothionin	32 ± 4	30 ± 2	38	29
β-purothionin	39 ± 5	33 ± 2	35	31

results and those of the visible excitation study (Table II), involving very different aspects of the Raman spectrum, is quite encouraging. In other cases the two methods can be expected to give different results because of their different concentration requirements, i.e., in cases where secondary structure is affected by aggregation. The dilute samples appropriate for UVRR spectroscopy assure that complications associated with unwanted aggregation are minimized.

On the other hand, the composite nature of the amide II UVRR intensity limits the method to the major structural components. The amide II frequency is relatively insensitive to the peptide conformation, but the amide I and III frequencies show a wide range for different conformations (Frushour & Koenig, 1975). Recent progress in deconvoluting the amide I band in Fourier-transform infrared spectra indicates that minor structural elements (β-turns etc.) can also be determined if the signal/noise is sufficiently high (Byler et al., 1986). Similar results may be possible from UV Raman spectroscopy if the quality of the data can be improved sufficiently. Unfortunately, as noted above, the amide I band is not strongly enhanced in UVRR spectra at excitation wavelengths so far attainable. The amide III band is stronger, but it is overlapped (Copeland & Spiro, 1985; Copeland et al., 1985; Rava & Spiro, 1985) by resonance-enhanced bands of phenylalanine, tyrosine, and tryptophan, which are present in most proteins, making deconvolution difficult. For the moment, the amide II band intensity gives the best prospect for determining secondary structure via UVRR spectroscopy.

ACKNOWLEDGMENTS

We are indebted to Professors F. G. Prendergast and J. Valentine for providing protein samples.

REFERENCES

Bensing, J. L., & Pysh, E. S. (1969) *Chem. Phys. Lett. 4*, 120.
Billeter, M., Braum, W., & Wuthrich, K. (1982) *J. Mol. Biol. 155*, 321.
Blundell, T., Dobson, G., Hodgkins, D., & Marcola, D. (1972) *Adv. Protein Chem. 26*, 279.
Brahms, S., & Brahms, J. (1980) *J. Mol. Biol. 138*, 149.
Byler, D. M., Brouillette, J. N., & Susi, H. (1986) *Spectroscopy 1*, 29.
Campbell, I. D., & Dwek, R. A. (1984) *Biological Spectroscopy*, pp 225–277, Benjamin/Cummings, Menlo Park, CA.
Cantor, C. R., & Schimmel, P. R. (1980) *Biophysical Chemistry*, Part II, Freeman, New York.
Chinsky, L., Jolles, B., Laigle, A., & Turpin, P. Y. (1985) *J. Raman Spectrosc. 16*, 235.
Copeland, R. A., & Spiro, T. G. (1985) *Biochemistry 24*, 4960.
Copeland, R. A., & Spiro, T. G. (1986) *J. Am. Chem. Soc. 108*, 1281.
Copeland, R. A., Dasgupta, S., & Spiro, T. G. (1985) *J. Am. Chem. Soc. 107*, 3370.
Creighton, T. E. (1983) *Proteins, Structure and Molecular Properties*, pp 159–197, Freeman, New York.
Dickerson, R. E., & Geis, I. (1983) *Hemoglobin*, p 31, Benjamin/Cummings, Menlo Park, CA.
Dickerson, R. E., Takano, T., Eisenberg, D., Kallai, O. B., Samson, L., Cooper, A., & Margoliash, E. (1971) *J. Biol. Chem. 246*, 1511.
Dudik, J. M., Johnson, C. R., & Asher, S. A. (1985a) *J. Phys. Chem. 89*, 3805.
Dudik, J. M., Johnson, C. R., & Asher, S. A. (1985b) *J. Chem. Phys. 82*, 1732.
Fodor, S. P. A., Rava, R. P., Copeland, R. A., & Spiro, T. G. (1986) *J. Raman Spectrosc.* (in press).
Fodor, S. P. A., Copeland, R. A., & Spiro, T. G. (1987) *J. Am. Chem. Soc.* (in press).
Frushour, B. G., & Koenig, J. L. (1975) *Adv. Infrared Raman Spectrosc. 1*, 35–97.
Glasoe, P. K., & Long, F. A. (1960) *J. Phys. Chem. 64*, 188.
Harada, I., & Takeuchi, H. (1986) in *Advances in Spectroscopy: Biological Systems* (Clark, R. J. H., & Hester, R. E., Eds.) Wiley, New York (in press).
Johnson, C. R., Ludwig, M., O'Donnell, S., & Asher, S. A. (1984) *J. Am. Chem. Soc. 106*, 5008.
Krimm, S., & Bandkar, J. (1986) *Adv. Protein Chem.* (in press).
Lipert, J. L., Tyminski, D., & Desmeules, J. J. (1976) *J. Am. Chem. Soc. 98*, 7075.
Lowey, S. (1965) *J. Biol. Chem. 240*, 2421.
Mayne, L. C., Ziegler, L. D., & Hudson, B. (1985) *J. Phys. Chem. 89*, 3395.
Momii, R. K., & Urry, D. W. (1968) *Macromolecules 1*, 372.
Onari, S. (1970) *J. Phys. Soc. Jpn. 29*, 528.
Painter, P. C., & Koenig, J. L. (1976) *Biopolymers 15*, 241.
Parker, F. S. (1983) *Applications of Infrared, Raman, and Resonance Raman Spectroscopy in Biology*, pp 83–153, Plenum, New York.
Peterson, D. L., & Simpson, W. T. (1957) *J. Am. Chem. Soc. 79*, 2375.
Rava, R. P., & Spiro, T. G. (1985) *Biochemistry 24*, 1861.
Richardson, J. S., Thomas, K. A., Rubin, B. H., & Richardson, D. C. (1975) *Proc. Natl. Acad. Sci. U.S.A. 72*, 1349.
Rosenheck, K., & Doty, P. (1961) *Proc. Natl. Acad. Sci. U.S.A. 47*, 1775.
Sugawara, Y., Harada, I., Matsuura, H., & Shimanouchi, T. (1978) *Biopolymers 17*, 1405.

Tinoco, I., Jr., Halpern, A., & Simpson, W. T. (1962) in *Polyamino Acids, Polypeptides, and Proteins* (Stahmann, M. A., Ed.) pp 147–160, University of Wisconsin Press, Madison, WI.
Trulson, M. O., & Mathies, R. A. (1986) *J. Chem. Phys. 84*, 2068.
Walton, A. G. (1981) *Polypeptides and Protein Structure*, pp 172–188, Elsevier, New York.
Wand, A. J., & Englander, S. W. (1986a) *Biochemistry 25*, 1100.
Wand, A. J., & Englander, S. W. (1986b) *Biochemistry 25*, 1107.
Wetlaufer, D. B. (1962) *Adv. Protein Chem. 17*, 303.
Williams, R. W. (1983) *J. Mol. Biol. 166*, 581.
Williams, R. W., & Teeter, M. M. (1984) *Biochemistry 23*, 6796.

Interaction of Polymyxin B Nonapeptide with Anionic Phospholipids†

Peter Kubesch,‡ Joan Boggs,§ Liliana Luciano,‖ Günter Maass,‡ and Burkhard Tümmler*,‡

Abteilung Biophysikalische Chemie and Abteilung Zellbiologie und Elektronenmikroskopie, Medizinische Hochschule, D-3000 Hannover 61, West Germany, and Research Institute, Department of Biochemistry and of Clinical Biochemistry, The Hospital for Sick Children, Toronto, Ontario, Canada M5G 1X8

Received August 14, 1986; Revised Manuscript Received December 11, 1986

ABSTRACT: The interaction of polymyxin B nonapeptide (PMBN) and polymyxin B (PMB) with the anionic phospholipids phosphatidylserine (PS), dipalmitoylphosphatidylglycerol (DPPG), dipalmitoylphosphatidic acid (DPPA), and 1:1 mixtures (w/w) of DPPA and distearoylphosphatidylcholine (DSPC) was studied by calorimetry, electron spin resonance, and fluorescence spectrometry, electron microscopy, and fusion and leakage assays. The phase transition temperatures of DPPA and DPPG were very similar when bound to PMB or PMBN, indicating that the lipids are in a similar state when bound to the cationic peptides. Both PMB and PMBN caused the interdigitation of DPPG bilayers, suggesting that the penetration of hydrophobic side chains from a peptide bound electrostatically on the surface is sufficient to induce this phenomenon. Stopped-flow experiments revealed that PMBN and PMB induced the fusion of small unilamellar PS and large unilamellar DPPA–DSPC vesicles. The aggregation of vesicles was found to be a diffusion-controlled process; the subsequent fusion took place with a frequency of 10^2–(5×10^2) s^{-1} for small vesicles and 1–100 s^{-1} for large vesicles. The freeze–fracture replicas of the PMB-treated vesicles displayed 12–50-nm depressions on several superimposed bilayers, indicating the formation of stable lipid–PMB domains. Since the incubation with PMBN produced similar depressions only if the specimens were fixed, PMBN-induced domain formation seems to be a reversible rapid process. The differences in the phospholipid–peptide interactions are correlated with the differences in the physiological action of the antibiotic PMB and the nonbactericidal PMBN on the cell envelope of Gram-negative bacteria.

The cationic peptide polymyxin B nonapeptide (PMBN)[1] is a derivative of the antibiotic polymyxin B that lacks the fatty acyl part of the parent compound (Chihara et al., 1973). PMBN is not bactericidal; however, it sensitizes Gram-negative bacteria to other amphiphilic and hydrophobic compounds (Vaara & Vaara, 1983b–d; Viljanen & Vaara, 1984). In the presence of PMBN, Gram-negative bacteria become vulnerable to a wide range of antimicrobial agents to which they were previously insensitive because the restrictive permeability properties of the outer membrane are lost (Vaara & Vaara, 1983c; Nikaido & Vaara, 1985).

PMBN and polymyxins are compounds to which the presence of five or six 2,4-diaminobutyric acid residues confers a net positive charge. In the case of the polymyxins, binding to acidic molecules of the outer membrane of Gram-negative bacteria, including the lipid A region of lipopolysaccharide (LPS), is assumed to be the primary event of drug action (Teuber & Bader, 1976; Storm et al., 1977; Hancock, 1984). Binding studies with isolated LPS (Bader & Teuber, 1973; Schindler & Osborn, 1979) and with lipid monolayers (Rosenthal et al., 1976; Teuber & Miller, 1977; El Mashak & Tocanne, 1980) and bilayers (Hartmann et al., 1978; Sixl & Galla, 1979, 1980, 1982; Galla & Trudell, 1980; Ranck & Tocanne, 1982; Boggs & Rangaraj, 1985) have revealed a high and specific affinity of the polymyxins for lipopolysaccharides and acidic phospholipids.

†This work was supported by a grant from the Deutsche Forschungsgemeinschaft. This paper is dedicated to Dr. Manfred Eigen on the occasion of his 60th birthday.

‡Abteilung Biophysikalische Chemie, Medizinische Hochschule, Hannover.
§Research Institute, The Hospital for Sick Children, Toronto.
‖Abteilung Zellbiologie and Elektronenmikroskopie, Medizinische Hochschule, Hannover.

[1] Abbreviations: CD, circular dichroism; CF, 5-carboxyfluorescein; DPA, dipicolinic acid; DPH, diphenylhexatriene; DPPA, 1,2-dipalmitoyl-*sn*-glycero-3-phosphatidic acid; DPPG, 1,2-dipalmitoyl-*sn*-glycero-3-phosphoglycerol; DSPC, 1,2-distearoyl-*sn*-glycero-3-phosphocholine; LPS, lipopolysaccharide; PMB, polymyxin B; PMBN, polymyxin B nonapeptide; PG, phosphatidylglycerol; PS, phosphatidylserine; TES, *N*-[tris(hydroxymethyl)methyl]-2-aminoethanesulfonic acid; T_m, midpoint temperature of a phase transition; EDTA, ethylenediaminetetraacetic acid; DSC, differential scanning calorimetry; Hepes, *N*-(2-hydroxyethyl)piperazine-*N*′-2-ethanesulfonic acid; ESR, electron spin resonance; Tris, tris(hydroxymethyl)aminomethane; MICs, minimum inhibitory concentrations.

0006-2960/87/0426-2139$01.50/0